eLIFE elifesciences.org

SHORT REPORT

Figures and figure supplements

Adaptation of hydroxymethylbutenyl diphosphate reductase enables volatile isoprenoid production

Mareike Bongers *et al*

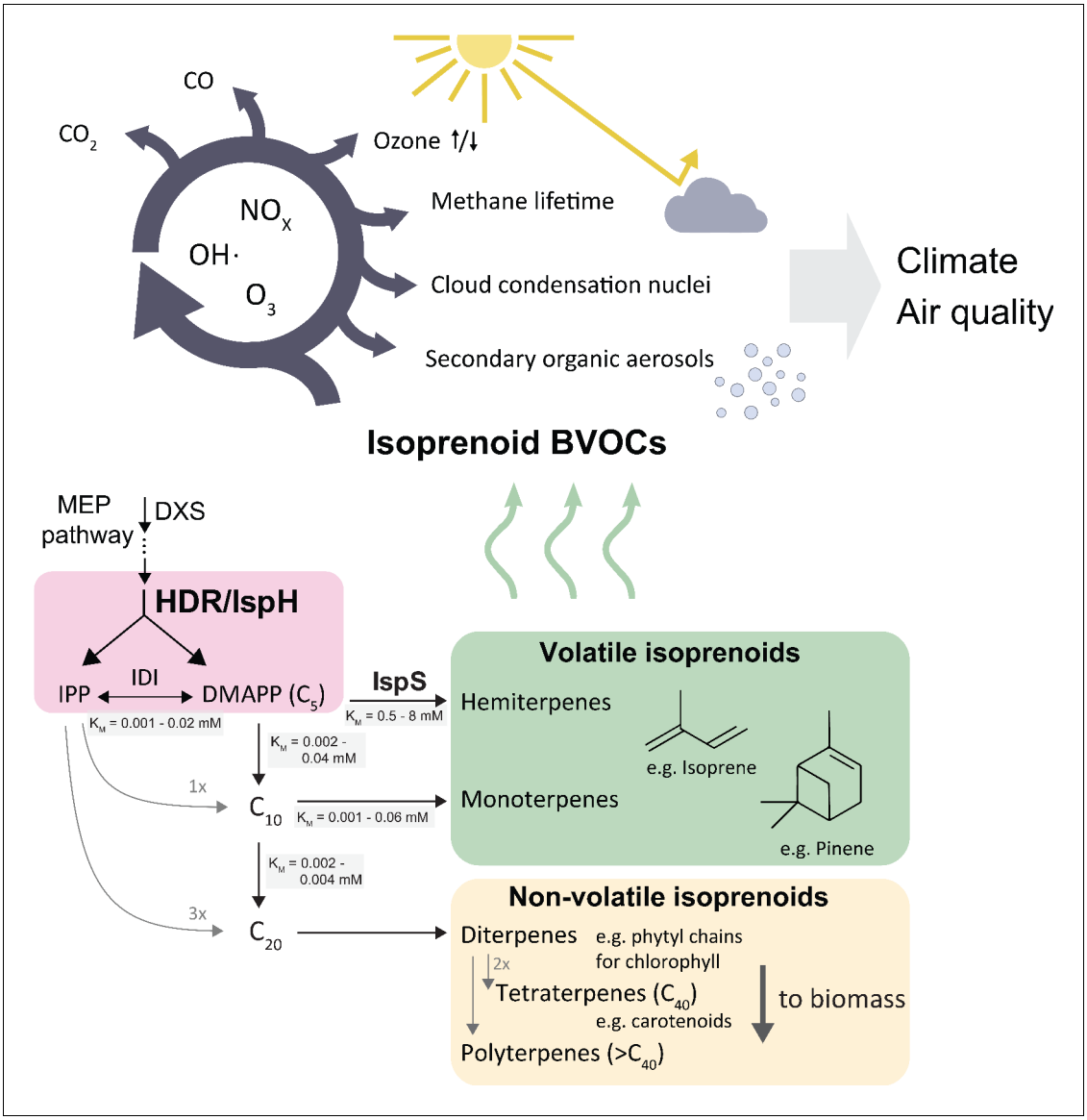

Figure 1. Simplified scheme of the plastidic MEP pathway, important volatile isoprenoids, and their atmospheric reactions. The MEP pathway makes IPP and DMAPP simultaneously through the action of HDR (pink box), and produces the bulk of volatile isoprenoids, contributing >80 % of total BVOCs (***Sindelarova et al., 2014***) . Non-volatile isoprenoids are essential and synthesised by all organisms, while volatile isoprenoid production is non-essential and highly species-dependent. The cytosolic MVA pathway contributes most sesquiterpenes (<3 % of BVOCs), but is omitted here for clarity. Emitted volatile isoprenoids are rapidly oxidised, resulting in complex atmospheric photochemistry impacting aerosol and cloud condensation nuclei formation, extension of methane residence time, ozonolysis as well as surface-level ozone formation in the presence of mono-nitrogen oxide (NO_x) pollutants (***Wennberg et al., 2018***). BVOCs, biogenic organic volatile compounds; DMAPP, dimethylallyl pyrophosphate; DXS, deoxyxylulose synthase; IDI, isopentenyl diphosphate isomerase; IPP, isopentenyl pyrophosphate; IspS, isoprene synthase; HDR, hydroxymethylbutenyl diphosphate reductase.

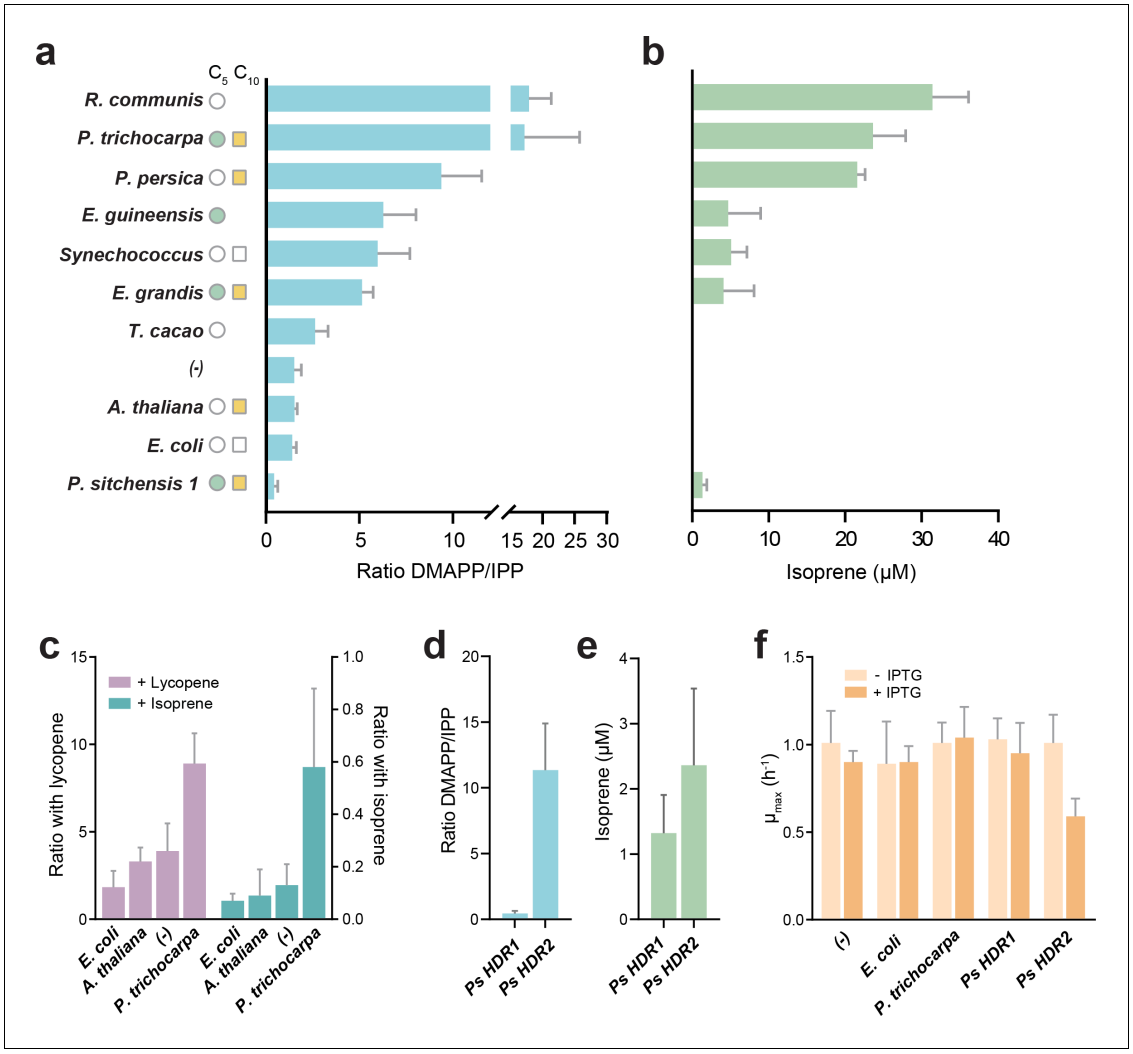

Figure 2. DMAPP:IPP ratio and isoprene production with different HDR enzymes. (**a**) In vivo ratio of DMAPP:IPP measured via LC-MS/MS in *E. coli* overexpressing *HDR* genes from different species, in the genetic context of *dxs* and lycopene biosynthetic pathway overexpression. Filled circles and squares indicate that the HDR source species natively emits C_5 or C_{10} isoprenoids. Open symbols indicate no emission, and no symbol indicates no data or conflicting data. (**b**) Isoprene production in *E. coli* when the HDR enzymes shown in panel (a) are overexpressed with *dxs* and an isoprene synthase. (**c**) Comparison of DMAPP:IPP ratios between selected *HDR*s co-expressed with *dxs* and with expression of either lycopene or isoprene as the metabolic sink. (**d**) Comparison of DMAPP:IPP ratios in *E. coli* overexpressing *Picea sitchensis* (*Ps*) *HDR1* or *HDR2* in the context of *dxs* and lycopene biosynthetic pathway overexpression. (**e**) Isoprene production in *E. coli* overexpressing *P. sitchensis HDR1* or *HDR2* along with *dxs* and an isoprene synthase. (**f**) The maximum specific growth rate (μ_{max}) of *E. coli* expressing selected *HDR*s in the context of *dxs* and lycopene biosynthetic pathway overexpression, with or without induction of *HDR* expression by addition of IPTG. All data shown as mean ± SD from ≥ 3 biological replicates; (-) indicates the control strain without *HDR* overexpression.

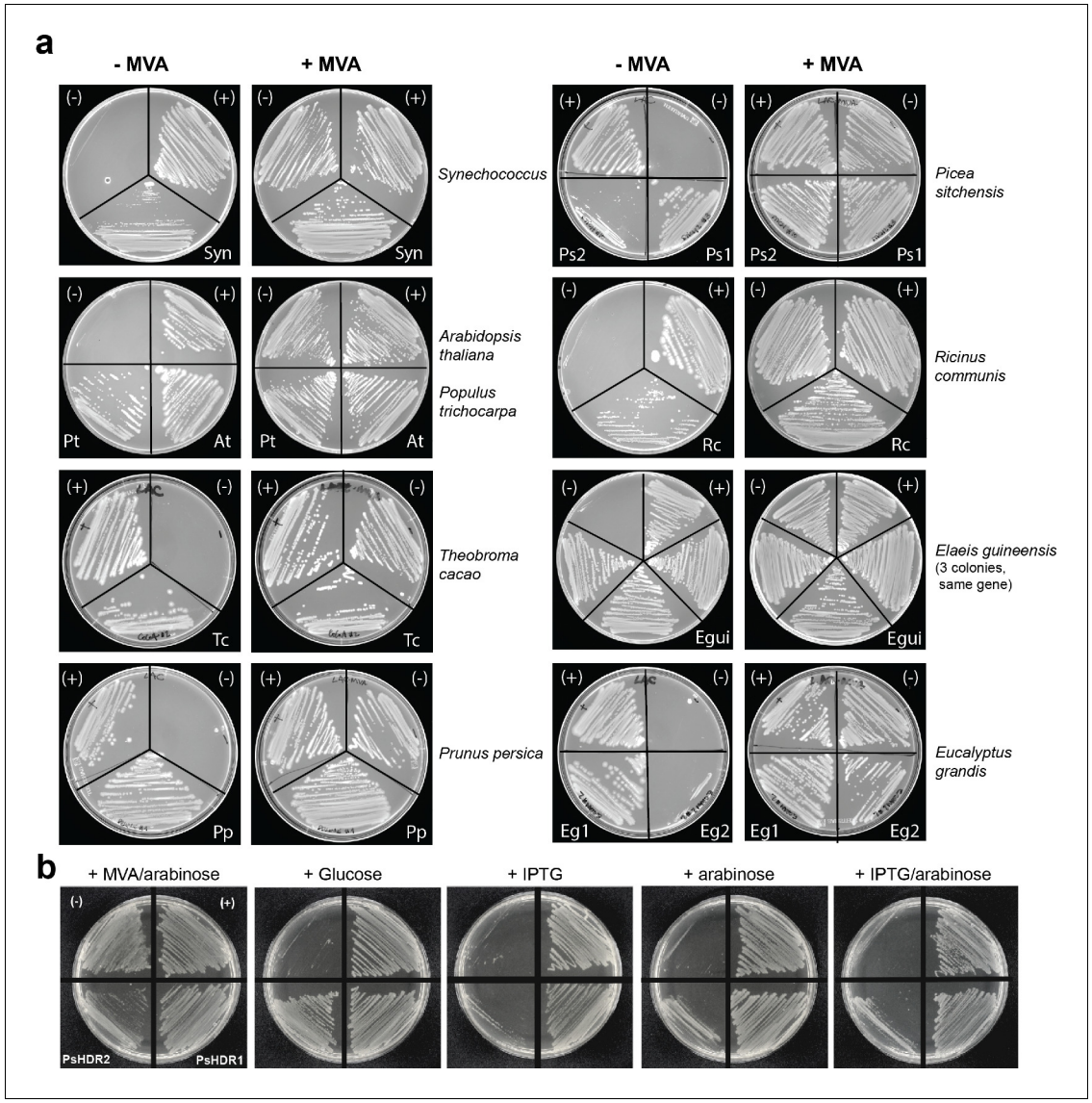

Figure 2—figure supplement 1. Complementation of lethal knockout of *ispH* in *E. coli* using different *HDR*s, and associated DMAPP toxicity. (**a**) An *E. coli* strain with a Δ*ispH* knockout and a heterologously expressed lower mevalonate (MVA) pathway depends on mevalonate for survival. When a functional *ispH/HDR* gene is expressed from a plasmid, growth can be restored in the absence of mevalonate. (-), empty vector negative control; (+), plasmid expressing *E. coli ispH* as a positive control. *E. grandis HDR2* and *P. trichocarpa HDR2* did not complement the Δ*ispH* knockout. MVA, mevalonate. (**b**) Toxicity of *P. sitchensis HDR2* in *E. coli* Δ*ispH*. Plasmid-encoded *HDR* genes are expressed from the *trc* promoter which can be induced with IPTG or partially repressed with glucose. *P. sitchensis HDR2*-associated toxicity can be alleviated by adding glucose to repress *HDR* expression, and is strongest under full IPTG induction. Arabinose, which induces the genomically encoded lower MVA pathway, including a heterologous *idi* gene, partly alleviates IPTG-induced toxicity. (-), empty vector negative control; (+), plasmid expressing *E. coli HDR* as a positive control. IPTG, Isopropyl β-D-1-thiogalactopyranoside; MVA, mevalonate.

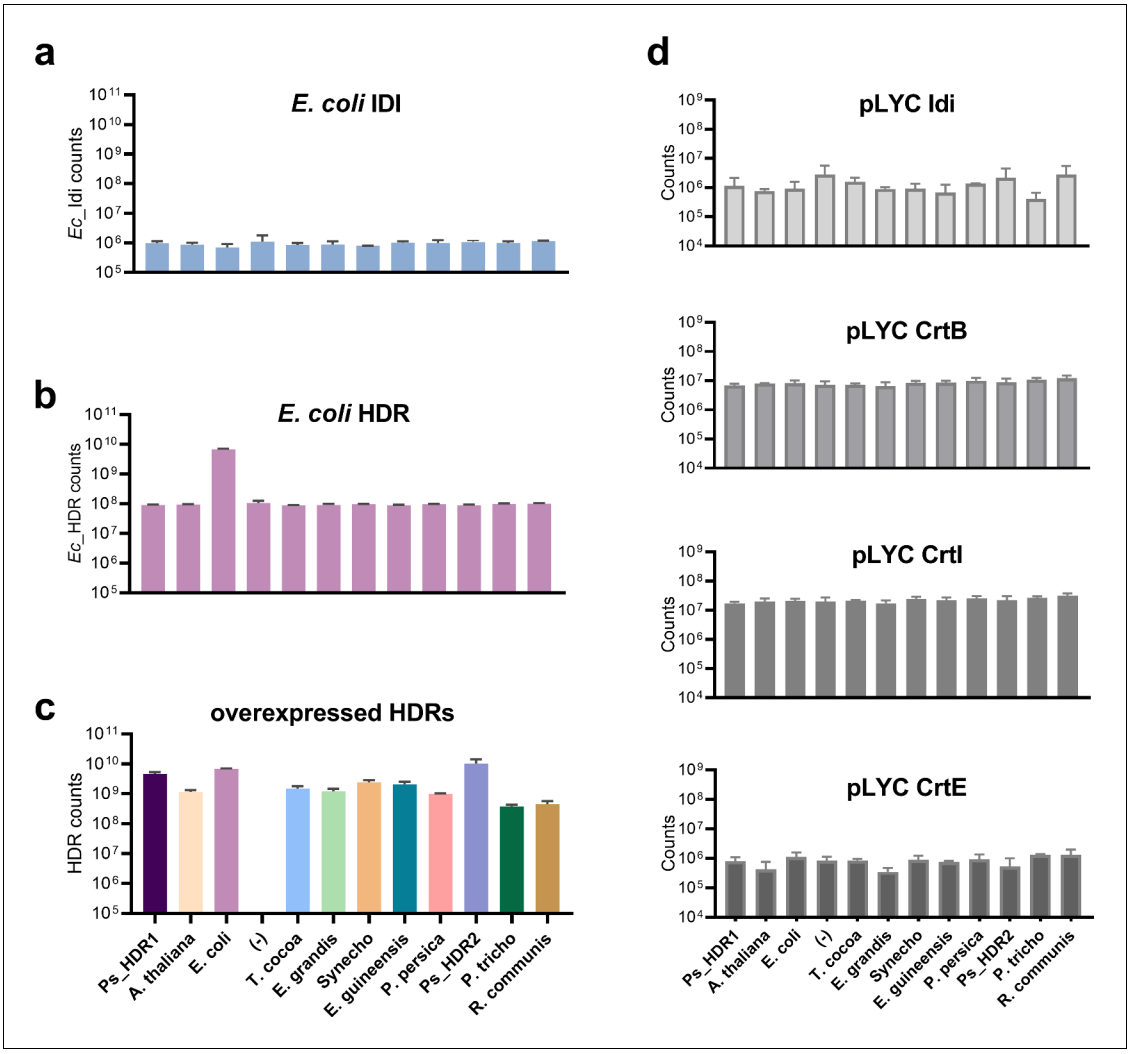

Figure 2—figure supplement 2. Protein quantification of IDI, HDR and the lycopene biosynthetic pathway. Relative protein abundance in *E. coli* overexpressing *HDR* genes from different species, in the genetic context of *dxs* and lycopene biosynthetic pathway overexpression. Proteins were quantified using untargeted proteomics via LC-MS/MS, and data represent the three most abundant peptide counts from each protein, normalized across all samples. (**a**) *E. coli* native Idi shows no significant difference between strains (one-way ANOVA, $p = 0.536$). (**b**) *E. coli* native HDR quantification. Only the *Ec*HDR overexpression strain is significantly different to the 'no HDR overexpression' (-) control (Welch's one-way ANOVA, $p = 0.0048$), no significant difference were observed between the other strains ($p \geq 0.743$). (**c**) Overexpressed, heterologous HDR proteins. Comparison of protein abundance between different HDR proteins is not possible due to a lack of shared tryptic peptides across all HDRs. Unique peptides for all overexpressed HDR proteins were detected with high abundance in the respective strains. (**d**) Plasmid-encoded lycopene biosynthetic pathway proteins. No significant differences were detected across strains for CrtI and CrtB (ordinary or Welch's ANOVA, respectively, $p \geq 0.05$). For Idi and CrtE, differences with $p < 0.05$ were detected between selected strains (e.g. *E. grandis* vs. *R. communis* CrtE $p = 0.034$); however, no significant differences were observed when comparing any of the strains to the negative control ($p \geq 0.78$ for Idi, Welch's one-way ANOVA; $p \geq 0.46$ for CrtE, ordinary one-way ANOVA). For Idi and CrtE, a total of only 3 peptides each were detected in our proteomics analysis, indicating low protein abundance and potentially explaining the higher variability between strains. Data represent means +/- SD from $n \geq 3$. All *p*-values were corrected for multiple hypothesis testing using Dunnett's method.

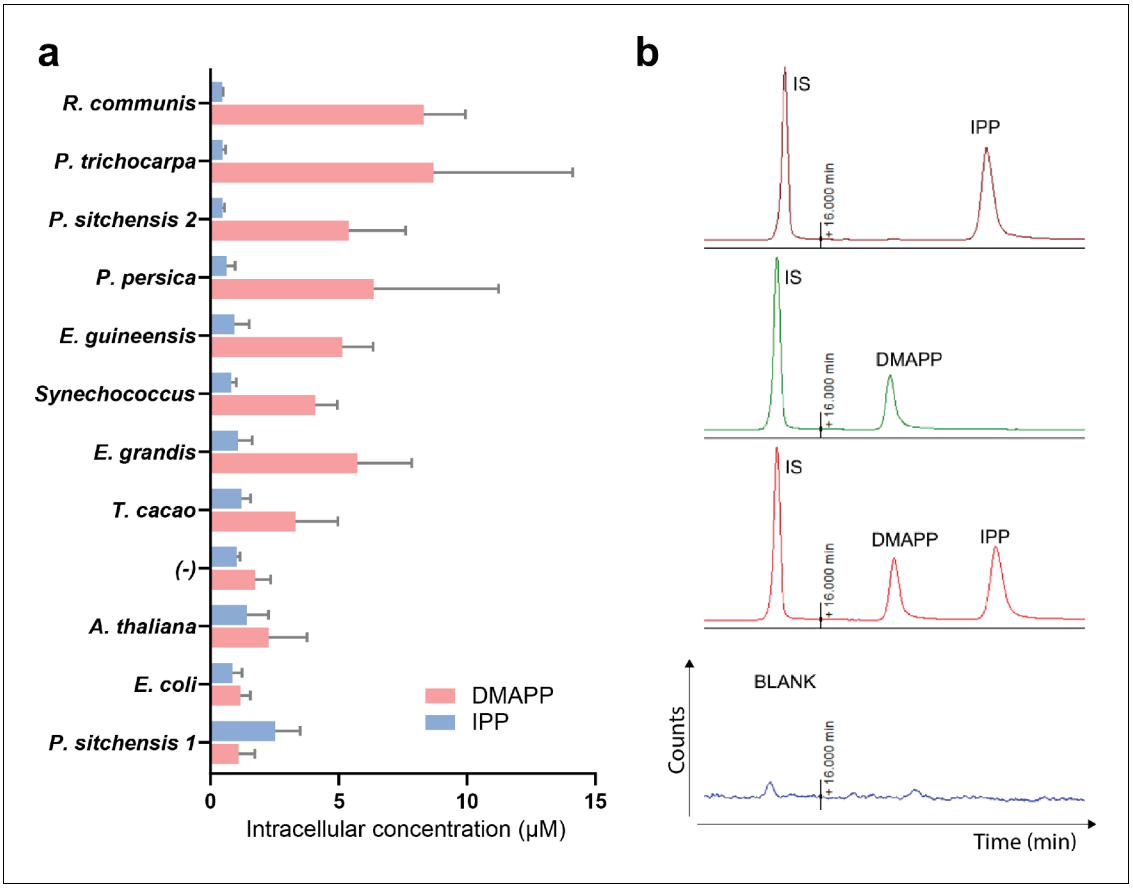

Figure 2—figure supplement 3. Quantification of DMAPP and IPP using LC-MS/MS. (**a**) Absolute quantification of intracellular DMAPP and IPP in *E. coli* overexpressing HDR genes from different species, in the genetic context of *dxs* and lycopene biosynthetic pathway overexpression. The difference in product ratio between HDRs at opposite ends of the graph is driven by both an increase in DMAPP and a decrease in IPP concentration. Data represent means +/- SD from n $\geq$ 3. (**b**) Representative chromatograms of matrix-matched calibration standards for DMAPP and IPP, including mevalonate-5-phosphate as internal standard (IS). Due to a slow, consistent drift in retention time over the HPLC column lifetime, no fixed retention times are given for DMAPP and IPP; however, with the presented method the analytes remain baseline-separated as shown here.

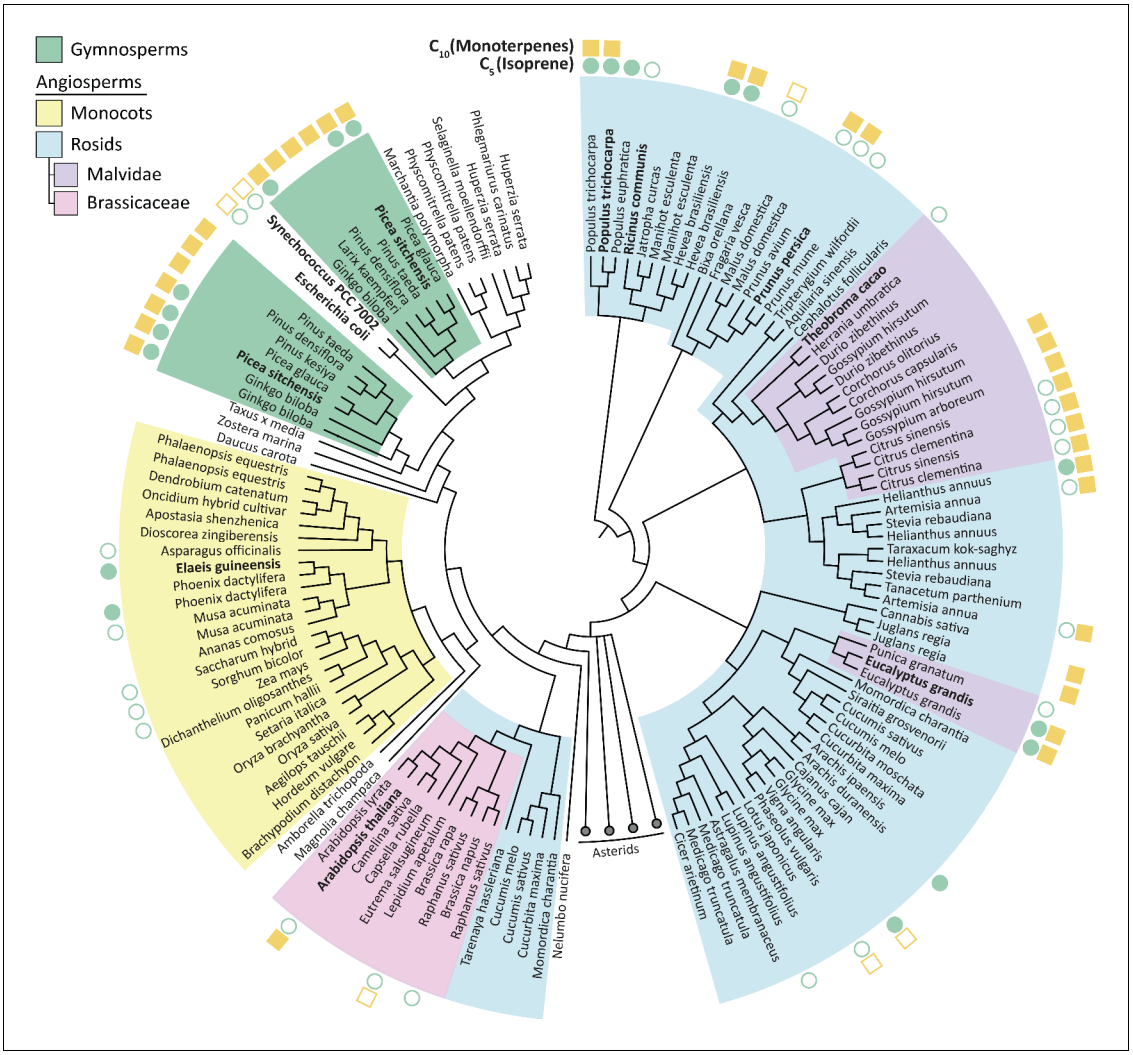

Figure 3. Phylogenetic tree of HDR proteins from land plants, the cyanobacterium *Synechococcus* and *Escherichia coli*. Where known, each species' C_5 (isoprene) and C_{10} (monoterpenes) emission spectra are shown (***Wiedinmyer et al., 2020***). High DMAPP-producing HDR proteins (from *P. trichocarpa*, *R. communis* and *P. persica*) cluster together based on high sequence similarity. Homologues within species, such as *P. trichocarpa*, tend to be highly similar; except for in gymnosperms where two separate groups of likely paralogous HDRs exist. Proteins analysed in this study are highlighted in bold. The Asterids clade is collapsed for clarity. Tree generated from BLAST sequence alignment with *A. thaliana* HDR against all land plants, using maximum likelihood phylogeny. Empty symbol, no volatile emission; filled symbol, volatile emission; no symbol, no or conflicting data available.